Laser-assisted bending by magnetic force

Besufekad N. Fetene[1], *Uday S. Dixit*[1], *João Paulo Davim*[2]

[1]*Department of Mechanical Engineering, Indian Institute of Technology Guwahati, Guwahati, India*
[2]*Department of Mechanical Engineering, University of Aveiro, Aveiro, Portugal*
E-mail: uday@iitg.ernet.in

Published in *The Journal of Engineering*; Received on 21st April 2017; Accepted on 8th June 2017

Abstract: In this study, a laser-assisted bending process is proposed, in which the external force is applied by magnets. The process can be used for bending the magnetic and non-magnetic materials. The experiments indicated that a large bend angle with reduced edge effect can be obtained by this process. The process was simulated by finite element method and a reasonable agreement was obtained between the experimental and simulated bend angles. It was experimentally observed that the micro-hardness after bending was greater than the original micro-hardness for mild steel as well as stainless steel work plates. In all the cases, micro-hardness reduced from laser-irradiated surface to opposite surface. Performance of the process as well as its ability to get accurately simulated bring out its potential of adaptability in industries.

1 Introduction

In the last three decades, there has been a lot of research on the use of a laser heat source for the forming of materials particularly for the bending of sheets, strips and tubes [1–3]. The use of laser for the bending can be classified into laser bending and laser-assisted bending. Laser bending is a non-contact process of bending, in which the heating by a laser beam generates thermal stresses that in turn govern the deformation of the material. On the other hand, in laser-assisted bending, the bending is carried out by the application of a load; the role of laser is to heat the material for reducing its flow stress and increasing the ductility. Researchers have demonstrated very wide application of laser bending. Friction-stir-welded aluminium alloy sheets [4], friction-stir-processed sheets [5], tailor machined blanks [6], aluminium components [7], titanium alloys [8], magnesium alloys [9], silicon [10], steel [11] and plastics [12] have been bent just with line heating by a laser beam. Lim and Lee [13] carried out line heating for forming the marine grade steel and studied the material properties after forming.

Laser-assisted bending has been successfully employed to bend brittle materials [14]. There are a variety of ways to carry out laser-assisted bending. Samm *et al.* [15] used a sapphire die transparent to solid-state and excimer laser beams to carry out the forming of the sheet metals. Kant and Joshi [16] used a roller to apply mechanical load that moves synchronously with a scanning laser beam. Yanjin *et al.* [17] simulated a laser-assisted bending, in which a load is applied at the free end of a cantilever sheet. The bend angle is enhanced when the direction of the load is consistent with the deformation direction in laser bending. On the other hand, Fetene *et al.* [18] hanged a load at the free end of a cantilevered sheet. In their experiments, the role of laser beam was mainly to reduce the flow stress of the material. Gisario *et al.* [19] investigated external force-assisted LaserOrigami (LO) bending of steel sheets to achieve three-dimensional (3D) cubes and stainless steel chairs by using a pneumatic actuator. LO technique was invented by Mueller *et al.* [20] to rapidly form 3D objects by folding a sheet by softening it at bend lines with the help of a defocused laser beam. In the original proposal of LO technique, the bending was accomplished by gravity, but any external force can be applied to accomplish it. Gisario *et al.*[19] applied an external force (pneumatic tool) and local and selective heating by irradiation with a high-power diode laser to bend Grade 2 CP titanium and AA 7075 T6 aluminium sheets.

So far, only mechanical loads have been applied in laser-assisted bending through physical contact. In this work, a magnetic force was applied along with laser heating. The magnetic force does not require physical contact and can reach inaccessible areas. Moreover, it can be easily controlled. Magnetic force has been used in metal forming processes. For example, Vivek *et al.* [21] carried out electromagnetic compression of steel tubes and also demonstrated that process can be simulated with a fair degree of confidence. In the age of competitive manufacturing, a process that can be simulated properly has better chances of adaptation by industry. Laser forming has been simulated numerically as well as analytically by a number of researchers. However, a review of the literature indicates that simulation of the process needs more maturity in terms of accuracy and computational efficiency [22, 23]. Respecting this requirement, apart from experimental investigation, finite element (FE) simulations of laser-assisted bending by magnetic force was also carried out.

2 Procedure of experiments

The magnetically assisted laser bending of mild steel and stainless steel plates was carried out. The magnetic force was measured experimentally for using the appropriate value of force in FE [FE method (FEM)] simulations. Afterwards, a number of experiments were carried out on a carbon dioxide (CO_2) laser machine. This section describes the experimental procedure.

2.1 Preparation of magnetic and non-magnetic plates

The samples were cut using CO_2 laser cutting machine into the required size of 200 mm × 120 mm for both magnetic and non-magnetic materials to carry out experiments. The rust and dust particles were removed from the surfaces by dissolving them in acetone. Graphite coating was used to enhance the absorptivity. For this work, mild steel was used as a representative magnetic material and stainless steel as a representative non-magnetic material. Samples were mounted as cantilever beams of 195 mm length; 5 mm length was used for clamping. Laser scanning was carried out along 120 mm width.

2.2 Measurement of magnetic force

Six neodymium permanent magnets, each of size 20 mm × 10 mm × 10 mm, were used in the experimental work. Pulling force strength of a magnet is affected by material properties, air gap (distance between magnet and work plate) and work plate thickness. Magnetic saturation in the plate limits the effective attractive force between the work plate and magnet. Fig. 1 shows a setup for measuring the magnetic force. One side of the work plate was fixed by a hinge and the other side hanged from a digital load

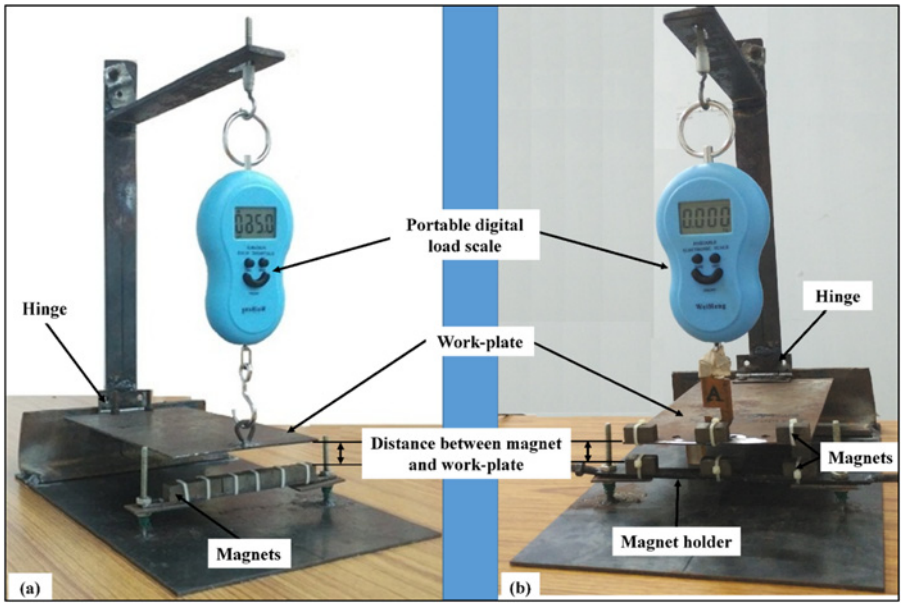

Fig. 1 *Experimental setup to measure the magnetic force on work plates made of*
a Mild steel
b Stainless steel

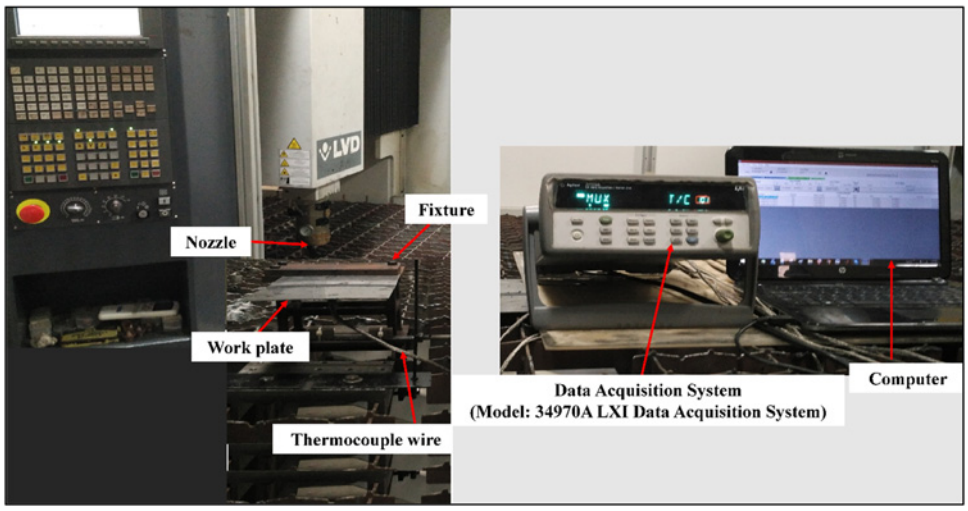

Fig. 2 *Experimental setup for measuring the temperature from bottom side of the plate*

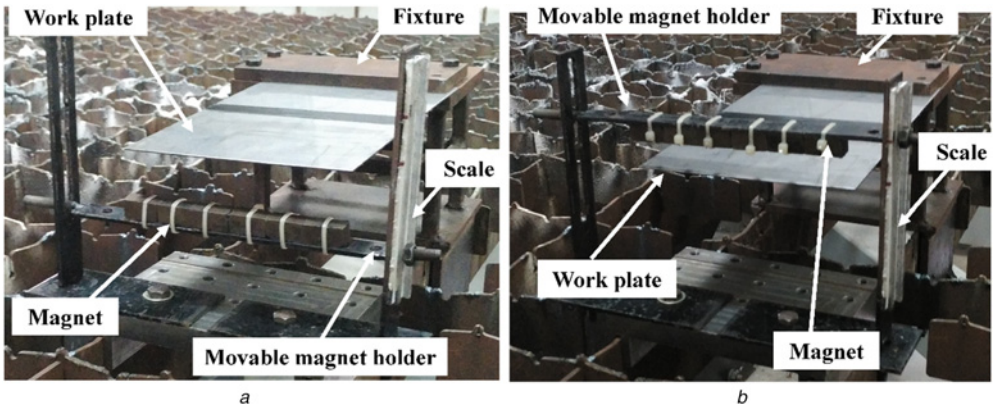

Fig. 3 *Photograph of the experimental setup for magnetic material (mild steel)*
a Magnet holder fixed at the bottom
b Magnet holder fixed at the top

doi: 10.1049/joe.2017.0145

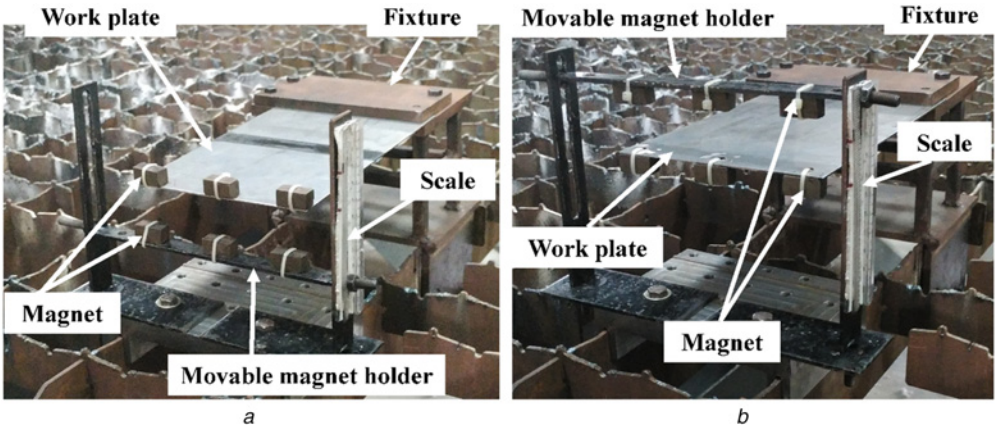

Fig. 4 *Photograph of the experimental setup for non-magnetic material (stainless steel)*
a Magnet holder fixed at the bottom
b Magnet holder fixed at the top

scale. The permanent magnet was attached below the work plate. For magnetic work material, the position of the magnet was set at the bottom of work plate without any contact between the work plate and magnet. In case of non-magnetic work material, three magnets were positioned at left, middle and right on the top surface of the work place along width direction and the other three were fixed on the magnet holder below the work plate. The opposite poles were facing each other such that there was attractive force between them. For both the cases, the net magnetic force was measured at the following gaps between the bottom surface of the work plate and the top surface of lower magnets: 20, 17.5, 15, 12.5, 10, 7.5, 5, 2.5 and 1 mm.

2.3 Measurement of the temperature during laser heating of work plate

Temperature at the bottom of the work plate was measured for laser power of 1 kW, laser spot diameter of 7.6 mm and scan speeds of 700 and 1100 mm/min. The K-type thermocouples (nickel chromium–nickel silicon) with an operating range from −40 to 1260°C and ± 1% accuracy were used for temperature measurement. The thermocouples were fixed at the bottom of the work plate through the thermocouple attachment unit (Dina-Weld TAU 100), 60 mm away from the start point of the scan line, i.e. at mid-width as shown in Fig. 2. The thermocouple wire end was connected to the Agilent Data Acquisition System (model: 349701A LXI data acquisition system). The data acquisition system was connected to computer, where the data was stored using Agilent bench link data logger software.

2.4 Experiments on laser-assisted bending

For laser-assisted bending, the plate was properly clamped on one side. The magnet holder was fixed either at the bottom or at the top side of the work plate as shown in Figs. 3 and 4 for the case of magnetic material (mild steel) and non-magnetic material (stainless steel), respectively. The magnet holder could easily be moved up and down through slot for varying the distance between magnets and work plate. The scale fixed at the side of the setup was used to measure the distance between the work plate and magnet. Before laser irradiation, the distances between work plate and magnet or between opposing magnets were kept constant and there was no bending just due to the magnetic force. The gap between the lower surface of the plate and the top surface of the lower magnets was 15 mm for non-magnetic material and 10 mm for magnetic material due to attractive force between magnets or between plate and magnet, respectively. The experiments were performed by using 2.5 kW continuous wave mode CO_2 laser (make: LVD, model: Orion 3015). The laser beam was irradiated in a direction parallel to free edge (along width) of clamped specimens at a distance of 100 mm away from free end. After the laser beam irradiation, the heated specimens were allowed to cool naturally.

Table 1 Experimental process parameters

Parameters	Symbol	Unit	Values
laser power	*P*	W	1000
laser beam diameter	*D*	mm	7.76
scan speed	*V*	mm/min	700, 800, 900, 1000 and 1100
magnet holder position	—	—	top, bottom and without magnet
material	—	—	mild steel and stainless steel

Table 2 Effect of element size on bend angle for laser power of 1000 W and scan speed of 1000 mm/min (number of divisions along length in each coarse zone fixed at 5)

Element size in refined zone, mm^3	Bend angle, deg	Screen time, s
2 × 2 × 0.333	0.67	12,400
1 × 1 × 0.333	0.72	18,000
0.5 × 1 × 0.333	0.78	21,350
0.5 × 0.5 × 0.333	0.8	25,350
0.5 × 0.5 × 0.25	0.81	36,000

Table 3 Mesh sensitivity analysis for coarse bias mesh in region between refined zone and free end for laser power of 1000 W and scan speed of 1000 mm/min (element size in refined zone: $0.5 \times 0.5 \times 0.333\ mm^3$, number of elements in region between refined zone and fixed end: 5)

Number of elements in coarse-biased mesh	Bend angle, deg	Screen time, s
5	0.8	25,350
10	0.83	27,120
15	0.85	29,235
20	0.87	34,330
25	0.87	39,115

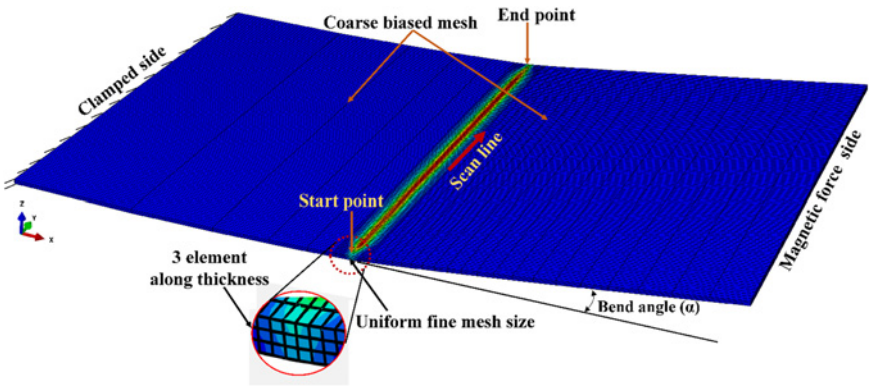

Fig. 5 *Mesh model of deformed plate of laser bending*

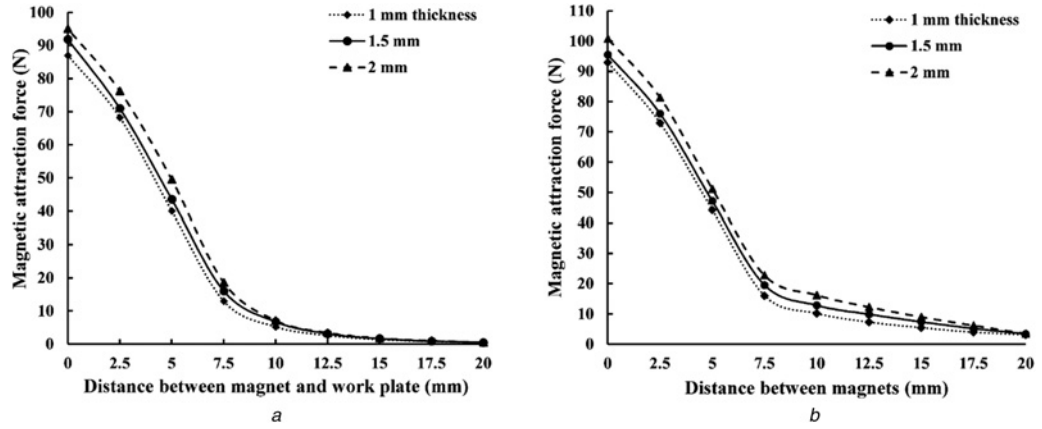

Fig. 6 *Variation of magnetic force with air gap for*
a Mild steel
b Stainless steel

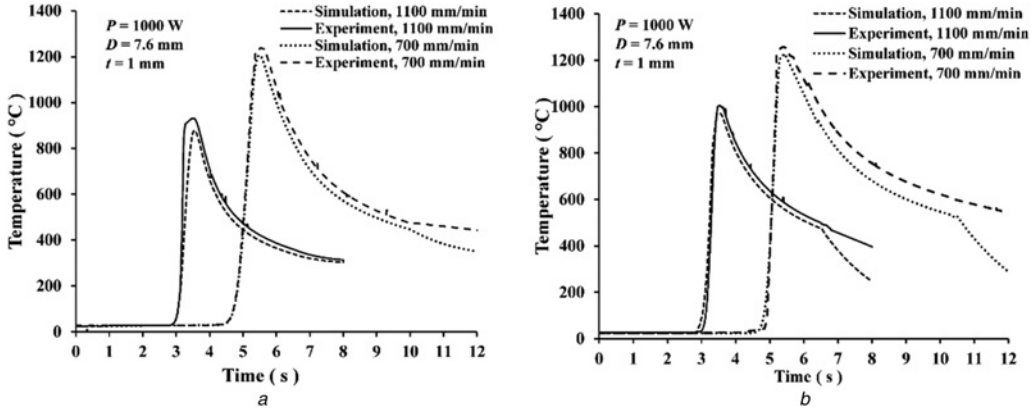

Fig. 7 *Simulated and experimental time histories of temperature for*
a Mild steel
b Stainless steel

The CO_2 laser has been utilised at different laser parameters. To validate the experiments of laser-assisted bending by applied permanent magnet force, the experiments were carried out at different process parameters listed in Table 1. Process parameters were laser power (P), beam diameter (D) and scan speed (V). The deformations of the laser-irradiated work plate samples were measured using a coordinate measuring machine and bend angles were estimated.

3 Details of simulation

Numerical simulations of laser as well as laser-assisted bending processes were performed to determine temperature distribution, edge effect and bend angles. A coupled thermo-mechanical process was conducted to simulate the laser-assisted bending process. Laser scanning was done at the mid-length of the work plate using FEM package ABAQUS® assuming work plate material as isotropic and no melting. Room temperature was set at 25°C.

doi: 10.1049/joe.2017.0145

Table 4 Magnetic attraction force for different materials and thicknesses

For non-magnetic material: distance between magnets (x) = 15 mm		
For magnetic material: distance between plate and magnet (x) = 10 mm		
Thickness, mm	Magnetic force, N	
	Mild steel	Stainless steel
1	5.5	5.6
1.5	5.6	7.4
2	6.94	9

3.1 Mesh sensitivity and time increment analysis

Fine mesh size was used in the laser-irradiated zone and coarse-biased mesh was used at rest of the places. Zhang *et al.* [24] recommended to take three elements in the thickness direction and four elements in a beam diameter (7.6 mm here). With this guideline, a mesh sensitivity analysis was carried out. Typical results are shown in Table 2. As a compromise between computational time and accuracy, an element size of 0.5 mm × 0.5 mm × 0.33 mm was found appropriate in the laser-irradiated zone.

Fetene *et al.* [18] observed that during laser-assisted bending, mostly the deformation takes place between the scan line and point of the application of the mechanical load. In the zone between the clamped side and laser-irradiated zone, the mesh sensitivity is small and it was considered sufficient to have five divisions along length in this zone. A relatively finer mesh was used in the zone between laser scan line and free edge. Table 3 shows the results of mesh sensitivity analysis for this zone. On the basis of this table, it was decided to use 20 divisions along length in this zone. In both the coarse mesh zones, the ratio of the division length of larger element to smaller element was 5:1.

Fig. 5 shows the final mesh with total three elements in the thickness direction. As per this meshing scheme, the total number of elements generated in the model was 32,400. The maximum time increment was taken as 0.01 s.

3.2 Mechanical and thermal boundary conditions

In mechanical analysis, necessary constraints are added according to the experimental fixture used in real experiments. The boundary conditions are zero translation and rotation motion at one side of the work plate, i.e. one side is fully constrained. The thermal load is given in the form of heat flux generated by the laser beam, which is applied on the top surface of the sheet metal. The heat flux density of moving laser beam is assumed to obey the normal distribution given by

$$q(x,\ y) = \frac{2\eta P}{\pi r^2} \exp\left\{-2\frac{\left(x^2+y^2\right)}{r^2}\right\}, \tag{1}$$

where q is the thermal heat flux density of laser beam, η is the absorptivity of the sheet material, P is the power of the laser and r is the radius of the laser beam on the surface of the plate.

The coefficient of absorption η was obtained in an inverse manner. The initial range of absorptivity was taken between 0.1 and 0.9. Bisection method was used to determine the particular value of absorptivity by comparing the simulation result with experimental result. It was decided to take absorptivity of material as 0.7 for both mild steel stainless steel with a graphite coating. Thermal and mechanical temperature-dependent properties were taken from the literature [24, 25]. However, the density of mild steel was taken as 7850 kg/m^3 for all the temperatures. For stainless, the density varied from 7320 to 7900 kg/m^3 in the range of temperatures encountered.

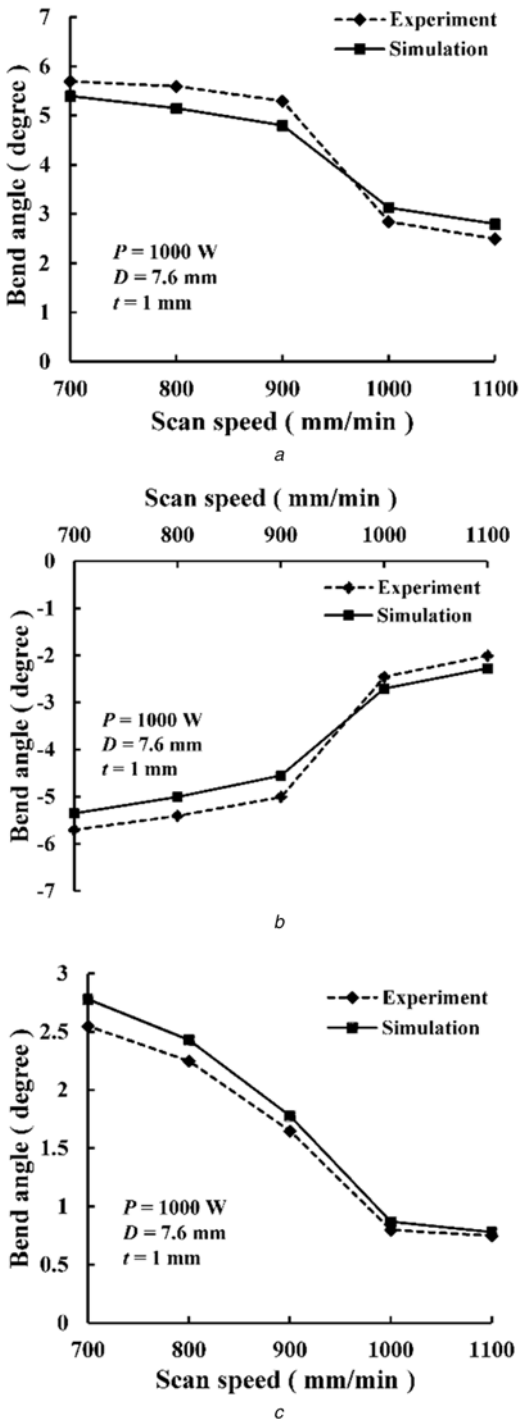

Fig. 8 *Bend angle result at various scan speeds for mild steel*
a Upward magnetic attractive force
b Downward magnetic attractive force
c Without magnetic force

Convective heat transfer takes place between the work plate and the surroundings. Newton's law of cooling provides

$$q = h(T_s - T_a), \tag{2}$$

where T_s is the surface temperature of the sheet, T_a (= 25°C) is the ambient temperature, q is the heat flux, h is the heat transfer coefficient, taken as 10 W/m^2 °C during heating. The cooling process was accelerated by taking a high value of h as described by Eideh [26] without sacrificing the accuracy of bend angle prediction.

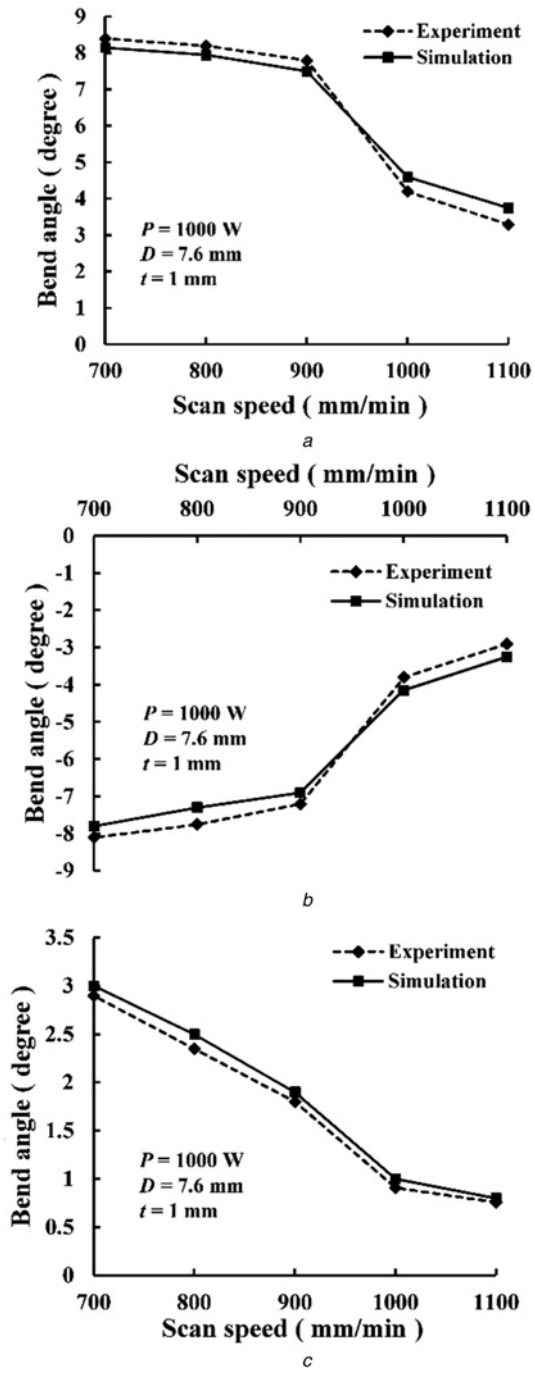

Fig. 9 *Bend angle result at various scan speeds for stainless steel*
a Upward magnetic attractive force
b Downward magnetic attractive force
c Without magnetic force

4 Result and discussion

In this section, experimental as well as simulation results are discussed. A comparison between the two results is made. The results clearly demonstrated the efficacy of the proposed process.

4.1 Measurement of magnetic force

Figs. 6*a* and *b* show the variation of magnetic attraction force with distance between the top surface of the magnet and bottom surface of the work plate for magnetic as well as non-magnetic material. The results are presented for three plate thicknesses: 1, 1.5 and 2 mm. It is observed that the magnetic attraction force increases slightly with the increase in the thickness of work plate and decreases as the distance between the top surface of the lower magnets and bottom surface of the work plate increases.

The following fifth degree expressions provide the magnetic force as a function of distance x (in millimetres) between the top surface of the lower magnets and the bottom surface of the plate:

$$F_{ms1} = 0.0005x^5 - 0.0276x^4 + 0.5479x^3 - 4.0169x^2 - 0.1717x + 86.899, \quad (3)$$

$$F_{ms1.5} = 0.0004x^5 - 0.0232x^4 + 0.4676x^3 - 3.4231x^2 - 1.938x + 91.674, \quad (4)$$

$$F_{ms2} = 0.0004x^5 - 0.0239x^4 + 0.5025x^3 - 3.9385x^2 - 0.257x + 94.718, \quad (5)$$

$$F_{ss1} = 0.0005x^5 - 0.0305x^4 + 0.5918x^3 - 4.2291x^2 - 0.3236x + 92.887, \quad (6)$$

$$F_{ss1.5} = 0.0005x^5 - 0.0302x^4 + 0.5881x^3 - 4.222x^2 - 0.1721x + 95.455, \quad (7)$$

$$F_{ss2} = 0.0006x^5 - 0.0319x^4 + 0.6183x^3 - 4.442x^2 + 0.1279x + 100.8, \quad (8)$$

where F with subscripts denotes the magnetic force in N. In the subscripts, the letters indicate the work material and the number indicates the plate thickness in millimetres. The coefficients of determination for (3)–(8) are 0.9989, 0.999, 0.9984, 0.9981, 0.9986 and 0.9985, respectively.

For simulation purpose, the force is considered corresponding to initial settings. Actually, the force varies during the process due to changing air gap between the plate and magnets as well change in the temperature of the plate. These two effects are of opposing nature; hence, assuming the constant value of force may not introduce much error. Table 4 shows the magnetic force at the fixed settings between the plates and magnets for plates of different

Table 5 Deviations between experimental and simulated bend angles (with downward magnetic force)

Material	Scan speed, mm/min	Thickness, mm	End angle, deg		
			Experiment	Simulation	Deviation, %
stainless steel	1100	1.5	−1.95	−2.20	12.8
	700	1.5	−6.75	−7.40	9.6
	1100	2	−1.6	−1.80	12.5
	700	2	−4.75	−5.20	9.5
mild steel	1100	1.5	−1.75	−2.00	14.3
	700	1.5	−2.95	−3.26	10.5
	1100	2	−0.2	−0.18	10
	700	2	−0.47	−0.52	10.6

doi: 10.1049/joe.2017.0145

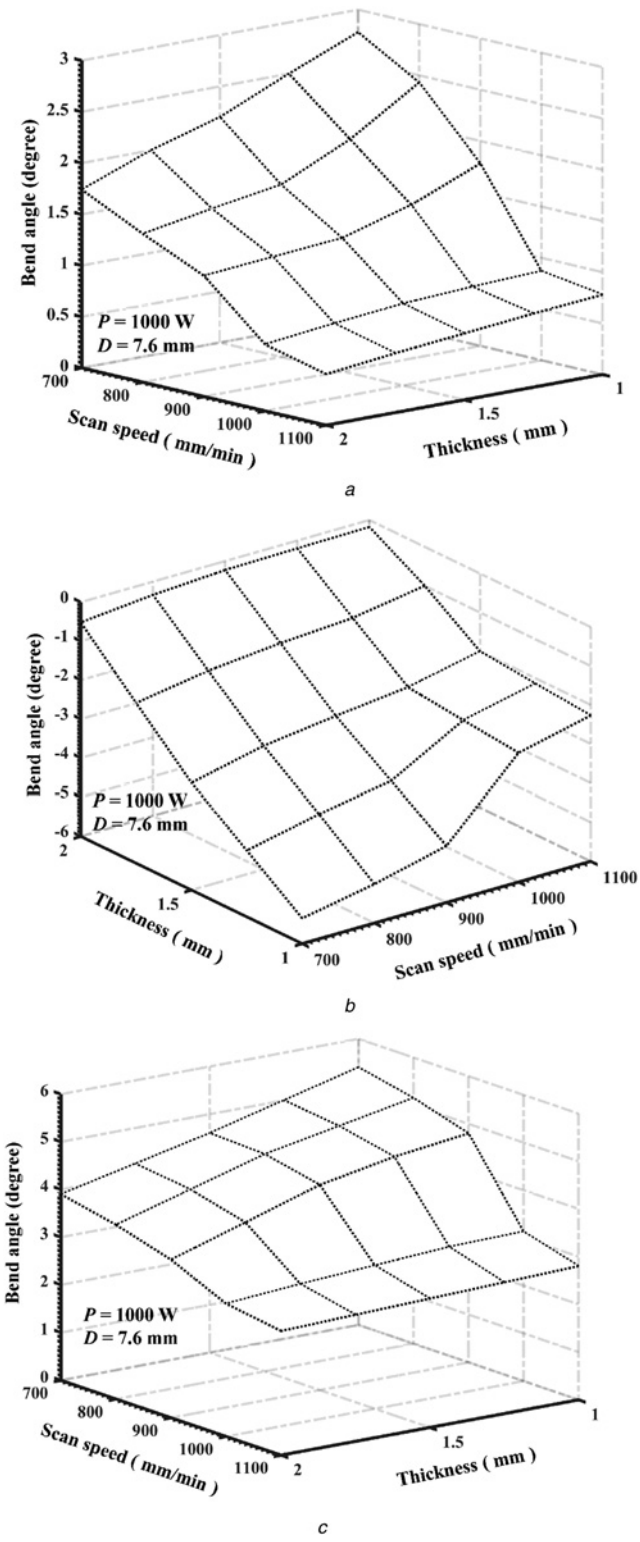

Fig. 10 *Laser bending of mild steel*
a Upward attractive force
b Downward attractive force
c Without magnetic force

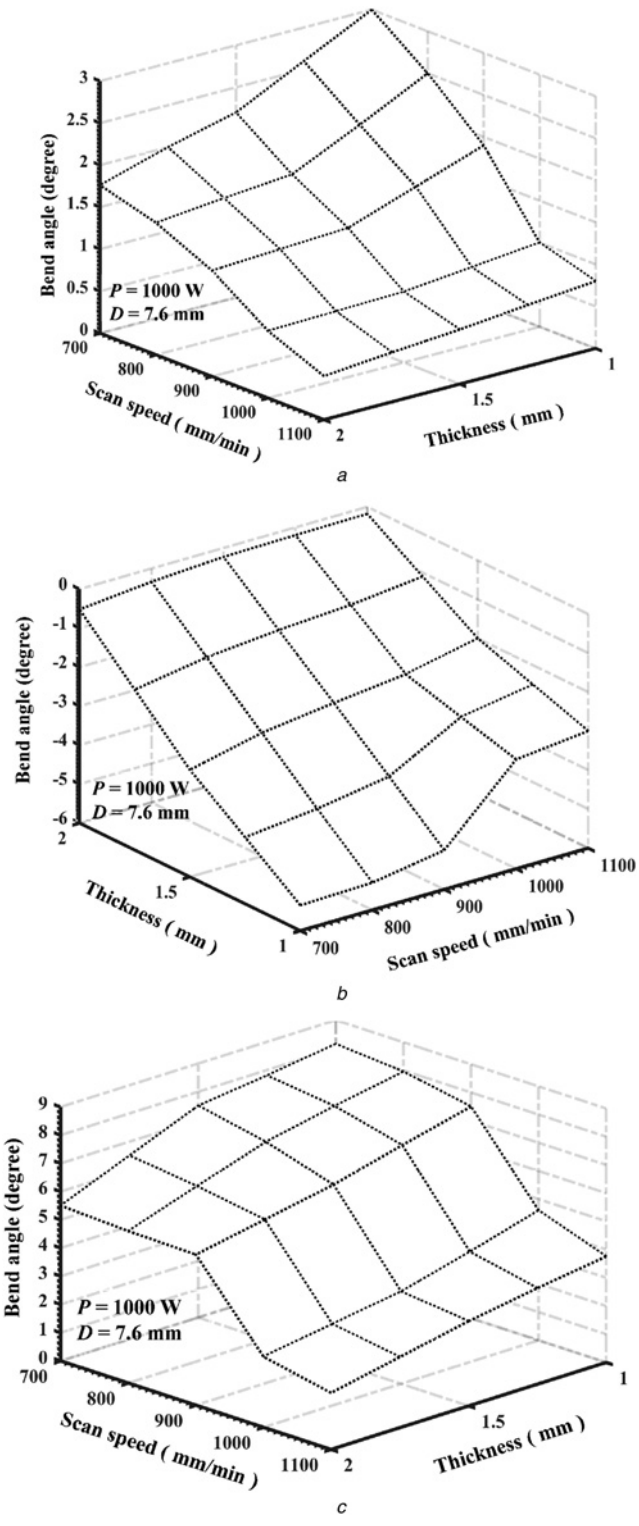

Fig. 11 *Laser bending of stainless steel*
a Upward attractive force
b Downward attractive force
c Without magnetic force

thicknesses. It is observed that the force increases with the increases in the thickness (t) of the plate.

4.2 Experimental and simulation results

For both mild steel and stainless steel, the experimental and simulation temperatures were evaluated at bottom side for scan speeds of 1100 and 700 mm/min. Figs. 7*a* and *b* show experimental and simulation temperature profiles at the bottom of the work plate and the centre of laser-irradiated line. There is a good agreement between experiment and simulation results. For mild steel, the peak temperature difference between experiment and simulations was 28.7 and 42.4°C for laser scan speeds of 700 and 1100 mm/min, respectively. The corresponding values for stainless steel are

doi: 10.1049/joe.2017.0145

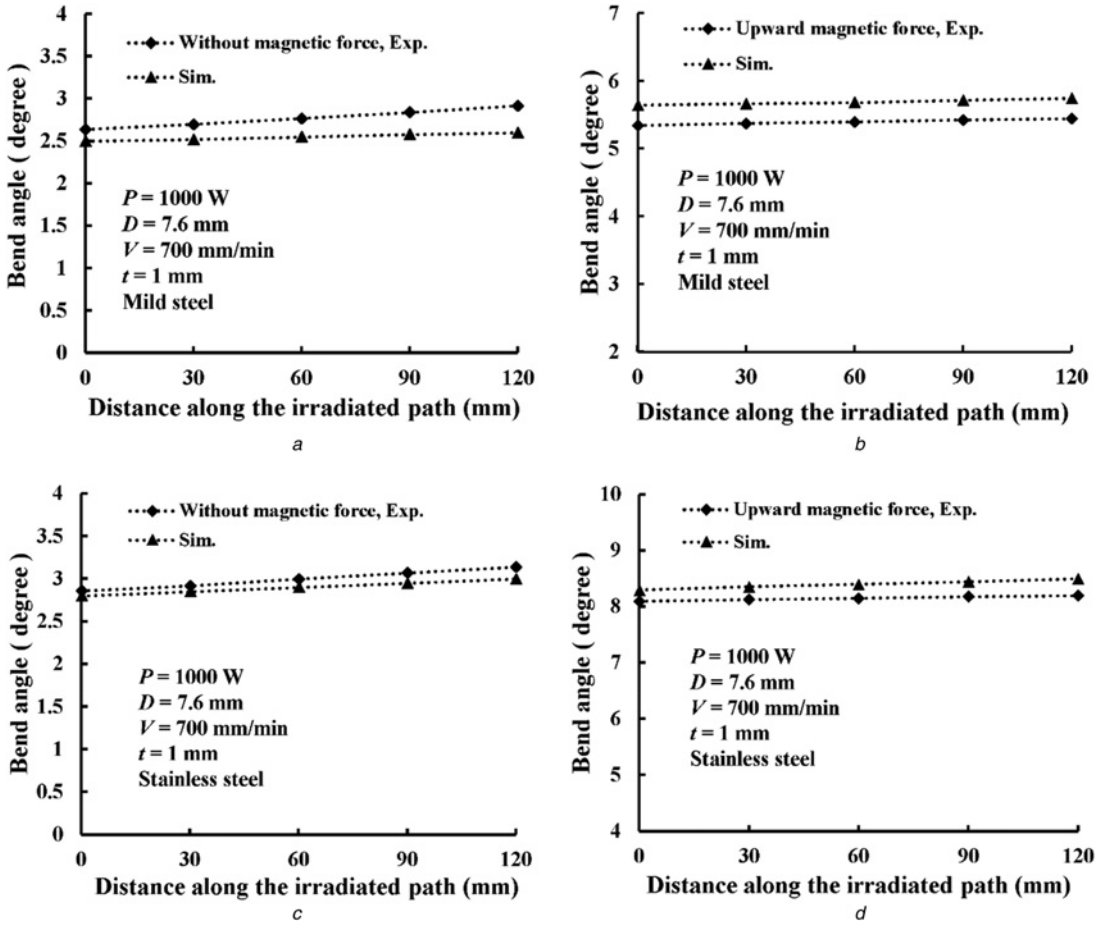

Fig. 12 *Variation of bend angle along the scan direction for*
a Mild steel plate without magnetic force
b Mild steel plate with upward magnetic force
c Stainless steel plate without magnetic force and
d Stainless steel plate with upward magnetic force

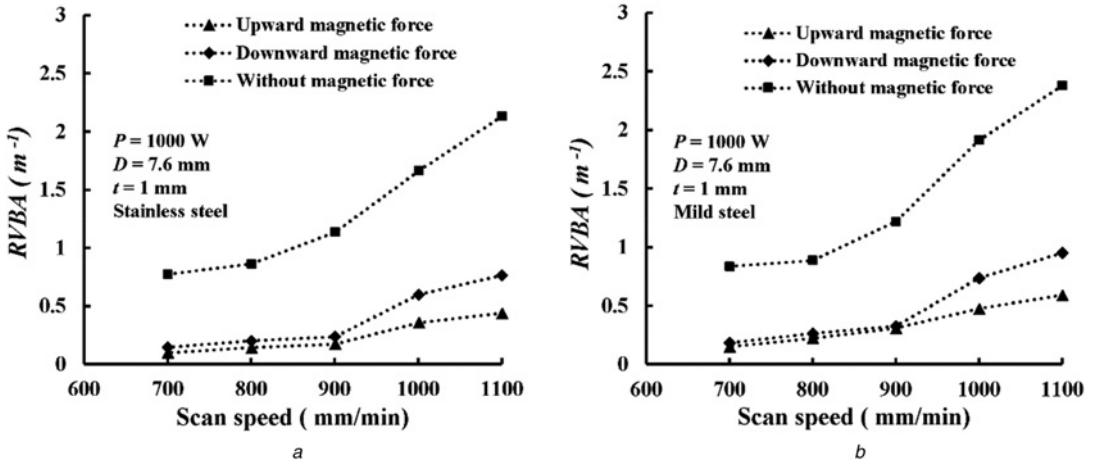

Fig. 13 *Effect of magnetic assisted bending on edge effect at different scan speeds for*
a Stainless steel work plate
b Mild steel work plate

26.5 and 33.8°C. These values are based on the absorptivity value of 0.7. As the deviation between experimental and simulation results is small in all the cases, this value of absorptivity was considered appropriate.

The work plate was bent due to the combined effect of laser beam irradiation and magnetic attractive force. Figs. 8 and 9 show the experimental and simulated bend angles for 1 mm thickness mild steel and stainless steel plates, respectively, at different scanning speeds. It is observed that the bend angle decreases with increase in scan speed for both materials. Figs. 8 and 9 show the results for the following three cases: (i) magnetic force direction upward, (ii) magnetic force direction downward and (iii) no magnetic force. In a single scan, the achievable bend angle is in the range $0.1 - 3°$ in the case of temperature gradient mechanism

doi: 10.1049/joe.2017.0145

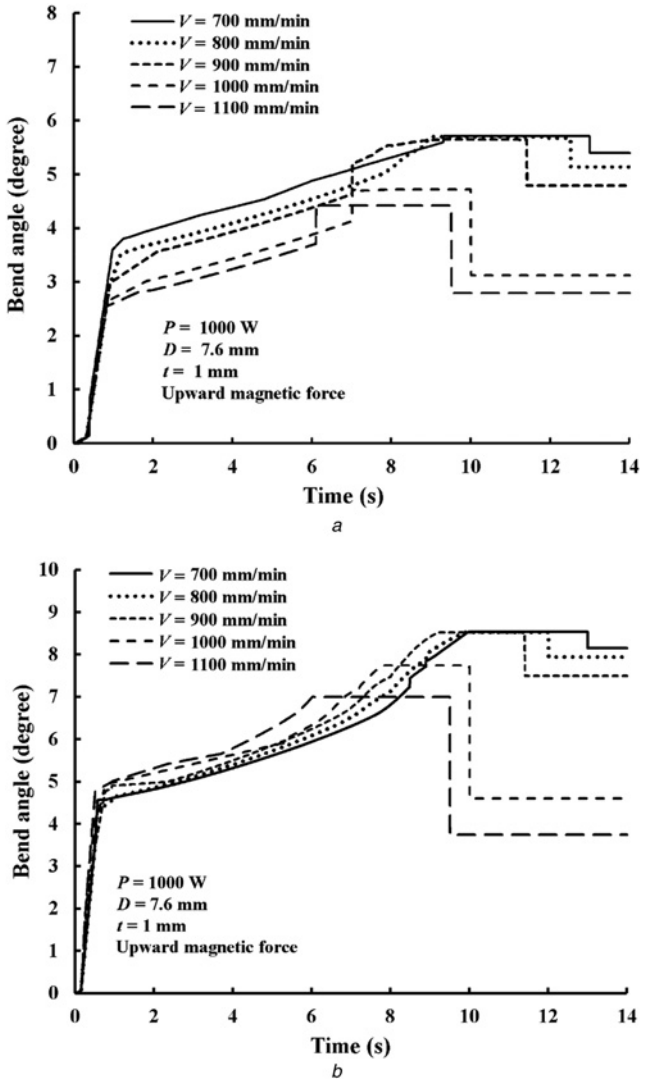

Fig. 14 *Evolution of bend angle with time in magnetically assisted bending as obtained by FEM simulation for*
a Mild steel
b Stainless steel at different scan speeds

(TGM) [27]. In TGM, the bend angle is achieved toward the laser source direction that is considered positive in this work. The results for laser bending without any external force are consistent with the literature. However, the application of magnetic force greatly enhances the bend angle.

Interestingly, the bend angle is greater when the magnetic force is upward than when it is downward. The first reason for this is that when the magnetic force is upward, TGM action and bending due to the force are in the same direction. The second reason is that due to upward movement of the plate, the spot diameter decreases, concentrating more heat in smaller area, which in turn enhances TGM action.

For mild steel work plate with upward force, the deviations between experimental and simulation results are 12, 9.82, 9.43, 8.04 and 5.26% for scan speeds of 1100, 1000, 900, 800 and 700 mm/min, respectively. The corresponding values are 13.5, 10.2, 9, 7.4 and 6.14% for downward magnetic force on mild steel plate. Without magnetic force, the corresponding deviations are 4, 8.75, 7.88, 8 and 9.02%. For stainless steel, the corresponding deviations are 13.64, 9.52, 3.85, 3.05 and 2.98% for upward magnetic force, 12.07, 9.21, 4.17, 5.81 and 3.7% for downward magnetic force and 5.26, 9.89, 5.56, 6.38 and 3.45% without magnetic force. Thus, there is a good agreement between experimental and simulation results.

For 1.5 and 2 mm thickness work plates, only two experiments were performed for each thickness at scan speeds of 700 and 1100 mm/min for both the materials. The magnetic force was acting downward. Table 5 shows the comparison of experimental results with the simulation results. A good agreement between the experiments and simulation reinforces the confidence in the modelling of the process. Figs. 10 and 11 show the surface plots showing the dependence of bend angle on scan speed and sheet thickness. These plots have been obtained from FEM simulations.

4.3 *Edge effect*

The variation of the bend angle along the laser scan direction (width direction) is called edge effect. Edge effect is defined in the literature as a relative variation in bend angle (RVBA) along the laser scanning line as

$$\mathrm{RVBA} = \frac{1}{w}\left(\frac{\alpha_{\max} - \alpha_{\min}}{\alpha_{\mathrm{ave}}}\right), \tag{9}$$

where $\alpha_{\max}$, $\alpha_{\min}$ and α_{ave} are the maximum, minimum and average bend angles along laser scan direction, respectively and w is the width of the work plate. The edge effect is more when the value of RVBA is higher, and vice-versa.

Fig. 12 shows the simulated and experiment bend angles along the laser scan directions. A good agreement is observed between them. To see the variation of edge effect with scan speed, simulations were carried out. Fig. 13 shows the simulated variation of edge effect with scan speed. The edge effect is less in laser-assisted bending compared with laser bending (without any magnetic force). This is due to better uniformity of the magnetic force. At low scan speed, the sheet got stuck with the magnets and was not allowed to move freely. In a way, magnets acted as fixture that restrained the movement of plate. Thus, uniform bend angle was obtained along the width direction.

4.4 *Simulation bend angle evolution with time*

In simulations, the magnetic force is taken corresponding to initial settings of the work plate and magnets. In practise, the bend angle evolves with time as shown in Fig. 14. It keeps increasing as the heating continues. Finally, there is some reduction in the bend angle due to spring back when the plate is removed from the setup. The spring-back effect is less at low scan speeds due to high temperature of the plate. Simulations presented in this work take into account the spring-back effect, but not the variation of magnetic force due to changing distance between the surface of the plate and magnets. It is also noted that as the gap between plate and magnets decreases causing an increase in the force, the temperature of the plate also increases that reduces the force. These two effects are of opposing nature and thus taking the force value at initial setting may not be in much error. However, a detailed analysis can be carried out in future.

4.5 *Micro-hardness*

The hardnesses of mild steel and stainless steel raw plates were 130 and 152 HV, respectively. Fig. 15 represents the variation of micro-hardness along perpendicular to laser scanning line of laser-irradiated plates for different scan speeds. Three readings were taken along thickness direction at 0.25, 0.5 and 0.75 mm from top (irradiation side) and average result is reported. As a result of laser scanning without magnetic force for mild steel, the average micro-hardness values were 180.4, 174.1, 168, 163.8 and 161.8 HV for scan speeds of 700, 800, 900, 1000 and 1100 mm/min, respectively, as shown in Fig. 15*a*. The corresponding values for stainless steel plates were 323.8, 295.5, 279.6, 259.2 and 249.8 HV, respectively (Fig. 15*b*). Obviously, the hardness is the

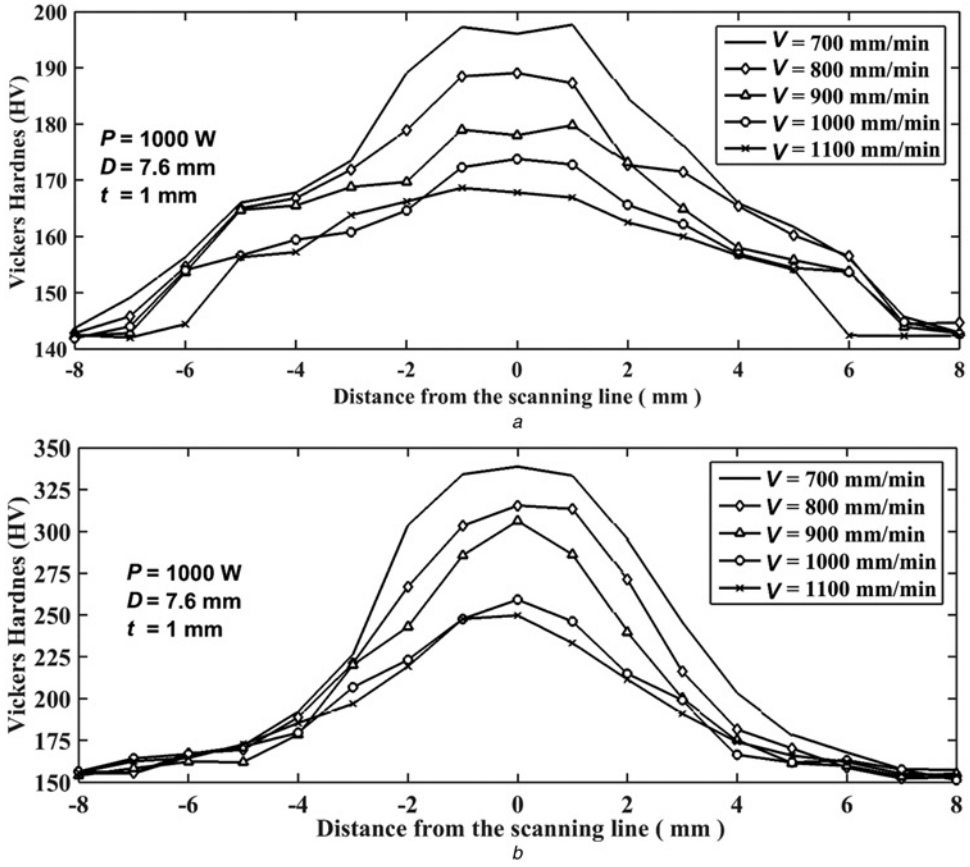

Fig. 15 *Average micro-hardness profile of laser-irradiated plate*
a Mild steel
b Stainless steel

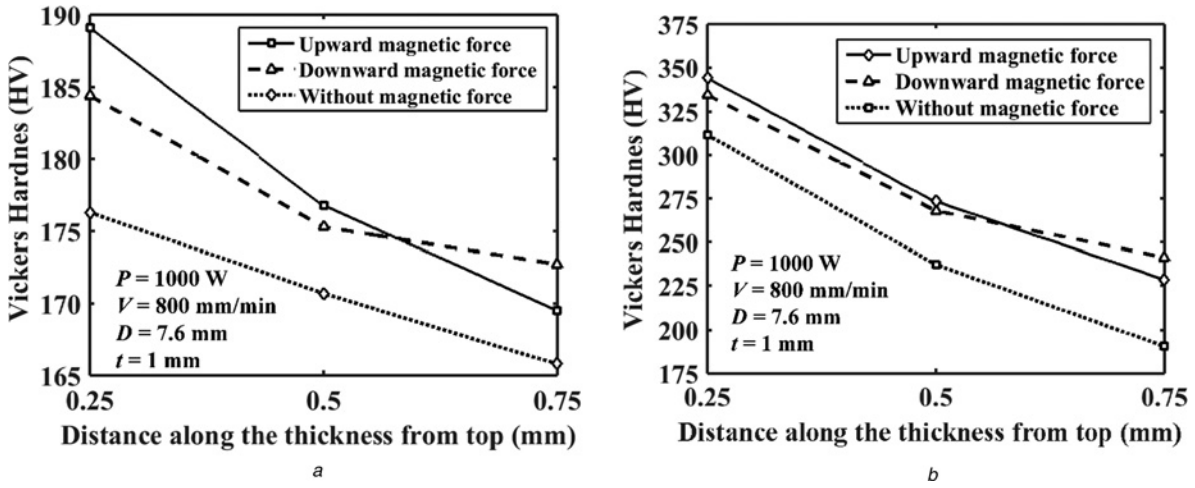

Fig. 16 *Average micro-hardness profile for downward magnetic force, upward magnetic force and without magnetic force for*
a Mild steel
b Stainless steel

maximum at and around the bend line. As the scan speed increases, the hardness decreases due to low amount of bending.

Fig. 16 shows the variation of hardness along the thickness direction. As a result of laser irradiation of mild steel, the hardness at 0.25 mm below the top of surface reached to 189.1, 184.4 and 176.3 HV for upward magnetic force, downward magnetic force and without magnetic force, respectively, as shown in Fig. 16*a*. The corresponding values for stainless steel plates were 344, 334.3 and 311.5 HV, respectively, as shown in Fig. 16*b*. Micro-hardness near the top surface of the work plate was greater than that near the bottom surface for both mild steel and stainless steel plates. This is due to more heating and corresponding heat treatment near the top surface. It was also observed that hardness near the bottom surface was more for bending with downward magnetic force compared with bending with upward magnetic force and without magnetic force. Bending with downward magnetic force creates relatively higher compressive strains at the bottom side, which is responsible for increasing the micro-hardness.

doi: 10.1049/joe.2017.0145

5 Conclusion

In this work, a manufacturing process is proposed to obtain large bend angles by laser-assisted bending with the application of magnetic force. The process can be used to bend magnetic as well as non-magnetic materials. The following are the salient findings from this work:

- Application of magnetic force could cause about two-fold enhancement in the bend angle. The bend angle was more when the directions of laser bending due to heating and the bending due to magnetic force coincided.
- The edge effect (the variation of bend angle along the width of the work plate) was also studied. The bend angle along width was higher at the end of the scan path. The edge effect increases with an increase in the scan speed. At low scan speed, the bend angle reached saturation as the plate got stuck with the magnets. This also reduced the edge effect. In general, the edge effect is lesser in magnetically assisted laser bending.
- Spring-back effect was lesser at low scan speed.
- Micro-hardness near the top surface of the work plate was greater than that near the bottom surface for mild steel as well as stainless steel work plates. Near the bottom surface, micro-hardness for laser bending with downward magnetic force was greater than that in laser bending with upward magnetic force or without any external force. This was due to relatively higher compressive strains on the bottom side for laser bending with downward magnetic force.

One encouraging observation about the proposed laser-assisted bending is that it could be simulated with reasonable accuracy. This is good for the acceptability of the process by industry. Simulations were carried out using an FEM package and the magnetic force was taken corresponding to initial settings. Effect of change in force due to deformation and temperature during the process was not taken into account. This may be considered in future.

6 References

[1] Dixit U.S., Joshi S.N., Kant R.: 'Laser forming systems: a review', *Int. J. Mechatronics Manuf. Syst.*, 2015, **8**, (3–4), pp. 160–205, doi: 10.1504/IJMMS.2015.073077

[2] Safdar S., Li L., Sheikh M.A., *ET AL.*: 'The effect of nonconventional laser beam geometries on stress distribution and distortions in laser bending of tubes', *ASME J. Manuf. Sci. Eng.*, 2007, **129**, (3), pp. 592–600, doi: 10.1115/1.2716715

[3] Folkersma G., Brouwer D., Römer G.: 'Microtube laser forming for precision component alignment', *ASME J. Manuf. Sci. Eng.*, 2016, **138**, (8), pp. 081012, doi: 10.1115/1.4033389

[4] Dixit U.S., Fetene B.N.: 'A finite element modelling of laser bending of friction stir welded aluminium 5052-H32 sheets', *Int. J. Mechatronics Manuf. Syst.*, 2016, **9**, (3), pp. 215–236, doi: 10.1504/IJMMS.2016.079589

[5] Fetene B.N., Dixit U.S., Liao H.: 'Laser bending of friction stir processed and cement-coated sheets', *Mater. Manuf. Process.*, 2017, pp. 1–7. Available at http://dx.doi.org/10.1080/10426914.2017.1279321, accessed April 2017

[6] Safari M., Mostaan H., Farzin M.: 'Laser bending of tailor machined blanks: effect of start point of scan path and irradiation direction relation to step of the blank', *Alexandria Eng. J.*, 2016, **55**, (2), pp. 1587–1594

[7] Labeas G.N.: 'Development of a local three-dimensional numerical simulation model for the laser forming process of aluminium components', *J. Mater. Process. Technol.*, 2008, **207**, (1), pp. 248–257

[8] Walczyk D.F., Vittal S.: 'Bending of titanium sheet using laser forming', *J. Manuf. Process.*, 2000, **2**, (4), pp. 258–269

[9] Kant R., Joshi S.N.: 'Thermo-mechanical studies on bending mechanism, bend angle and edge effect during multi-scan laser bending of magnesium M1A alloy sheets', *J. Manuf. Process.*, 2016, **23**, pp. 135–148

[10] Xu W., Zhang L.C., Wang X.: 'Laser bending of silicon sheet: absorption factor and mechanisms', *ASME J. Manuf. Sci. Eng.*, 2013, **135**, (6), pp. 061005–061005-7

[11] Gollo M.H., Mahdavian S.M., Naeini H.M.: 'Statistical analysis of parameter effects on bending angle in laser forming process by pulsed Nd:YAG laser', *Opt. Laser Technol.*, 2011, **43**, (3), pp. 475–482

[12] Okamoto Y., Miyamoto I., Uno Y., *ET AL.*: 'Deformation characteristics of plastics in YAG laser forming'. Fifth Int. Symp. Laser Precision Microfabrication, Nara, Japan, May, 2004, pp. 576–581

[13] Lim H.K., Lee J.S.: 'On the material properties of shell plate formed by line heating', *Int. J. Nav. Archit. Ocean Eng.*, 2017, **9**, (1), pp. 66–76

[14] Bammer F., Schuöcker D., Schumi T., *ET AL.*: 'A diode-laser-system for laser-assisted bending of brittle materials', *Adv. Opt. Technol.*, 2011, **2011**, Article ID 321807, pp. 1–4

[15] Samm K., Terzi M., Ostendorf A., *ET AL.*: 'Laser-assisted micro-forming process with miniaturised structures in sapphire dies', *Appl. Surf. Sci.*, 2009, **255**, (24), pp. 9830–9834

[16] Kant R., Joshi S.N.: 'Finite element simulation of laser assisted bending with moving mechanical load', *Int. J. Mechatronics Manuf. Syst.*, 2013, **6**, (4), pp. 351–366

[17] Yanjin G., Sheng S., Guoqun Z., *ET AL.*: 'Finite element modeling of laser bending of pre-loaded sheet metals', *J. Mater. Process. Technol.*, 2003, **142**, (2), pp. 400–407

[18] Fetene B.N., Shufen R., Dixit U.S.: 'FEM-based neural network modelling of laser-assisted bending', *Neural Comput. Appl.*, 2016, pp. 1–14, doi: 10.1007/s00521-016-2544-9

[19] Gisario A., Barletta M., Venettacci S.: 'Improvements in spring back control by external force laser-assisted sheet bending of titanium and aluminum alloys', *Opt. Laser Technol.*, 2016, **86**, pp. 46–53

[20] Mueller S., Kruck B., Baudisch P.: 'LaserOrigami: laser-cutting 3D objects'. Proc. SIGCHI Conf. Human Factors in Computing Systems, Paris, France, April 27 – May 2, 2013, pp. 2585–2592

[21] Vivek A., Kim K.H., Daehn G.S.: 'Simulation and instrumentation of electromagnetic compression of steel tubes', *J. Mater. Process. Technol.*, 2011, **211**, (5), pp. 840–850

[22] Eideh A., Dixit U.S., Echempati R.: 'A simple analytical model of laser bending process'. Chapter 1 in Lasers Based Manufacturing, Fifth Int. and 26th All India Manufacturing Technology, Design and Research Conf., Guwahati, India, December 2014, pp. 1–15

[23] Kant R., Joshi S.N., Dixit U.S.: 'Research issues in the laser sheet bending process', in Davim J.P. (ED.): 'Chapter 4 in materials forming and machining: research and development' (Woodhead Publishing, Cambridge, 2015), pp. 73–95

[24] Zhang L., Reutzel E.W., Michaleris P.: 'Finite element modeling discretization requirements for the laser forming process', *Int. J. Mech. Sci.*, 2004, **46**, (4), pp. 623–637

[25] Deng D., Murakawa H.: 'Numerical simulation of temperature field and residual stress in multi-pass welds in stainless steel pipe and comparison with experimental measurements', *Comput. Mater. Sci.*, 2006, **37**, (3), pp. 269–277

[26] Eideh A.: 'Determination of parameters during laser bending by inverse analysis'. MTech thesis, Department of Mechanical Engineering, IIT Guwahati, India, 2014

[27] Lawrence J., Schmidt M.J., Li L.: 'The forming of mild steel plates with a 2.5 kW high power diode laser', *Int. J. Mach. Tools Manuf.*, 2001, **41**, (7), pp. 967–977